

CFD Validation Of Forced And Natural Convection For The Open Phase Of IAEA Benchmark CRP - I31038

Abdalla Batta, Andreas Class
Karlsruher Institut für Technologie (KIT)
Hermann-von-Helmholtz-Platz 1,
76344 Eggenstein-Leopoldshafen Germany
abdalla.batta@kit.edu, class.andreas@kit.edu

Abstract – The goal of the IAEA Coordinated Research Project “Benchmark of Transition from Forced to Natural Circulation Experiment with Heavy Liquid Metal Loop” (CRP - I31038) is to develop Member State advanced fast reactor analytical capabilities for simulation and design using system, CFD, and subchannel analysis codes. Here we present CFD validation employing the commercial CFD code Star CCM+ applied to the fuel pin simulator for forced and natural convection cases in the open phase where experimental data is provided in the benchmark specification provided by ENEA (Italian National Agency for New Technologies, Energy and Sustainable Economic Development) for the NACIE-Up facility (NATURAL Circulation Experiment-UPgrade). Considered is the fuel pin simulator with 19 pins, each consisting of a preheated lower section and heated upper sections, respectively. Three configurations (i) all pins heated, (ii) inner 7 pins heated and (iii) asymmetric heating are studied. For each heating configuration data for forced and natural convection are provided. Here case (i) is studied. Temperatures at three planes are measured near the inlet, in the middle and near the end of the heated section, respectively. In addition, the axial temperature along the wall of one fuel pin simulator (in second row) is measured so that in total 67 thermocouples measure fluid and wall temperatures for validation purposes.

Our validation confirms that the thermohydraulic inside the fuel pin simulator can be simulated with a good accuracy. Applied is a polyhedral mesh with 2 prism layers, the k - ω SST model with all all-wall treatment and order unity y^+ values. Moreover, we performed a grid-sensitivity study and analysed the importance of conjugate heat transfer inside the fuel-pin simulators and the wrapper. Our studies indicate that it is possible to implement further simplifications without corrupting the accuracy of the simulation to reduce computational effort.

Keywords:

CFD, Liquid metal thermal hydraulic, Turbulence flow, Wire-wrapped bundle flow

I. Introduction

Benchmark studies are an essential tool to obtain confidence in simulation capabilities when large thermal loads occur. In particular, for nuclear applications, where failure can be accompanied with hazards to the public, maximum temperatures must be limited, and yet compact solutions must be achieved. The ENEA Brasimone Research Centre

(Italy) proposed for a benchmark exercise intended for system-alone, CFD/TH system code coupled simulations and stand-alone CFD simulations based on experimental results obtained from the 2017 campaign performed with the NACIE-UP (NATURAL Circulation Experiment- UPgraded) facility, [1], Fig. 1 shows the schematic representation of the NACIE-UP facility consists in a rectangular loop. It consists of two vertical pipes with an inner diameter of 62,68mm. The

working fluid is Lead Bismuth Eutectic (LBE), a fluid proposed for liquid metal cooled fast reactors. The experiments allow operation in the regimes of forced and mixed convection by combining a gas-lift pumping and buoyancy.

Inside the loop a fuel pin simulator (FPS) simulating a 19-pin fuel bundle is installed. Each pin-simulator contains an ohmic heater which can be activated individually, resulting in a maximum total heating power of 250 kW. The heated pins are arranged in 3 ranks with a triangular pitch (P) and with an active length $L_{active} = 600$ mm. The pins have a diameter $D_{pin} = 6.55$ mm and maximum wall heat flux close to 1 MW/m^2 . The wire diameter $d_{wire}=1.75$ mm. The pins are placed on a hexagonal lattice by a suitable wrapper, while spacer grids will be avoided thanks to the adoption of the wire spacer. The primary loop is insulated to ensure well-defined adiabatic experimental conditions.

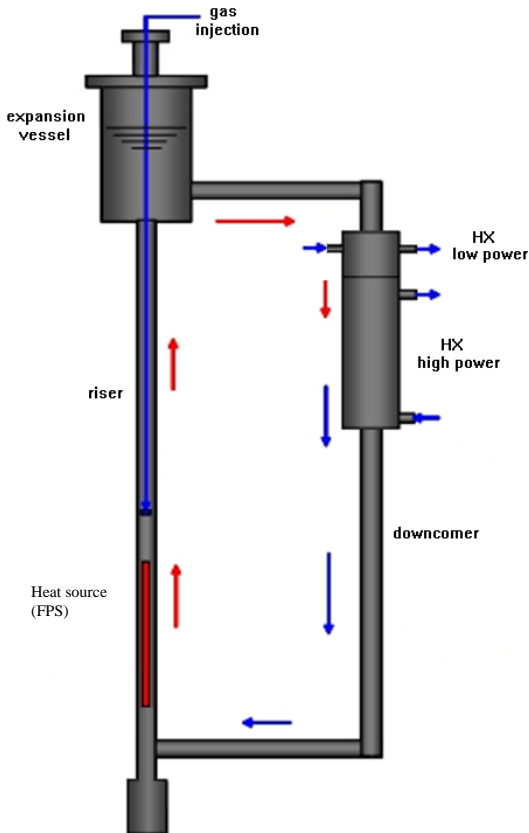


Fig. 1: Schematic representation of the NACIE-UP primary loop [1].

The 19 wire-spaced electrical pins are arranged in a triangular lattice by the hexagonal wrapper. The pitch to diameter ratio (P/D) is 1.2824. The total length, which includes the non-active length and the electrical

connectors, is 2000 mm. The dimensions of the FPS are summarized in table I

Table I : FPS design parameters [1]

Parameter	Value
D_{pin}	6.55 mm
P	8.4 mm
P/D	1.2824 mm
d_{wire}	1.75 mm
P_{wire}	262 mm
L_{total}	2000 mm
L_{active}	600 mm
$D_{H,nom}$	3.84 mm

In the open phase of the benchmark two symmetric heating configurations are studied. Test ADP10 corresponds to the activation of heating of all pins, while in the case ADP06 only the central and the second inner row are activated. The goal of the open phase is to set-up first simulations and choice of suitable models and computational parameters. In phase two a complex situation corresponding to asymmetrical heating is to be studied. Researchers do not receive any experimental data during the blind phase. The aim is to demonstrate that computational methods allow predictions once the researchers could validate their implementation for a small number of cases.

Note that each FPS heating configuration is experimentally investigated for a transient. The starting point of operation is a stationary forced convection state which is followed by a pump down-ramping resulting in a stationary natural-convection operation. Thus, each of the test cases ADP10, ADP 06 and ADP07 shown schematically in Fig. 2 acquired data for two steady states. In the current study we consider the case ADP10 for both forced and natural convection. Note that Fig.2 also indicates the numbering of rods and subchannels. In Fig. 3 details and dimensions of the vertical FPS are shown. The flow enters at the bottom of the test section to flow through an unheated preconditioner section located within the lower half of the vertical arrangement. The heated section follows the preconditioner section beginning at height $z=0$ mm, as shown in the figure.

In Fig. 4 positions of the thermocouples in the experimental setup are depicted. The experiment is equipped with three measurement planes (A,B and C) at heights 38mm, 300mm and 562 mm where both wall temperatures (i.e. red dots in the right figure) and subchannel temperatures (i.e. blue dots in the right figure) are collected.

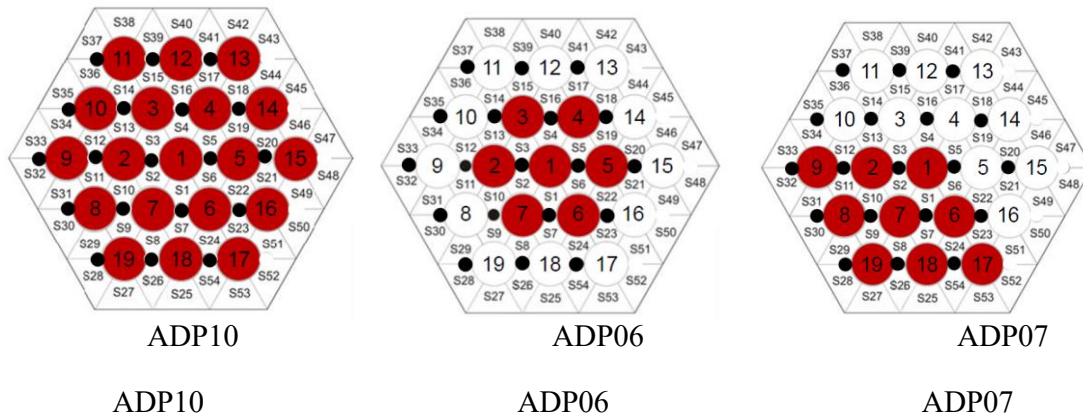


Fig. 2 Bundle cross section, benchmark test cases ADP10, ADP06 and ADP07, active pins (in red) during test.

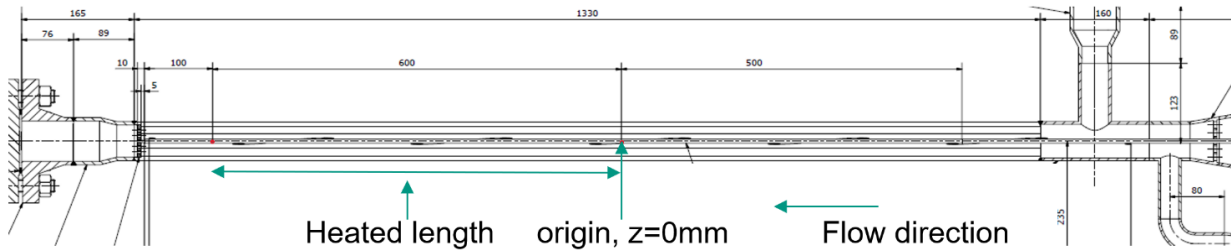


Fig. 3 CAD drawing of the test section and origin of the used coordinate system [1].

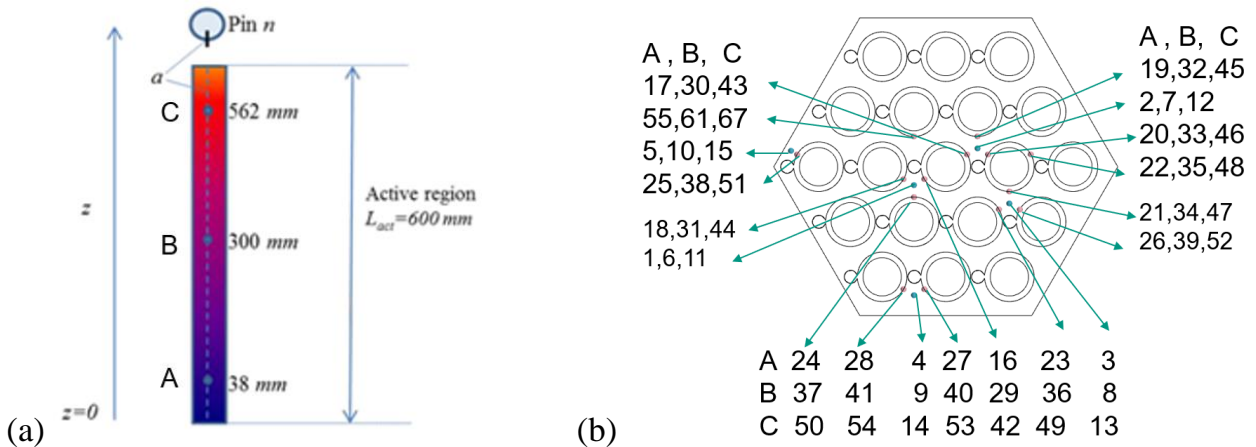


Fig. 4 (a) Location of planes for TC measurements in the test section (A at 38mm, B at 300mm and C at 562mm) (b) location and names of thermocouples in measurements planes.

In addition, rod 3 is equipped with 10 (plus 3 in the measurement planes) thermocouples to measure the axial surface temperature, TC number from 55 to 67, see Fig. 4. The 13 thermocouples on pin 3 are arranged inline. The temperature data at the thermocouples along with integral operational data serves as the benchmark data. The reader is referred to benchmark specifications in [1] for more details.

II. Benchmark specification (studied cases)

Table II contains the integral operational conditions of the steady state conditions 1 and 2, corresponding to forced and natural convection, respectively, case ADP10. The table also includes error estimates for the integral parameters. As forced convection is provided by the gas-lift pumping the LBE mass flow shows an error of up to 11%, this uncertainty with other ones are relevant for later

assessment of prediction capabilities. Moreover, the heating is not fully restricted to the heating section as the fuel pin simulators also show some heating in the preconditioning section. Consequently, the effective heating in the heated section Q_{eff} and the Q_{pre} in the preconditioning will be considered in the simulations. The Q_{tfm} is the power supplied for thermos-flow meter upstream of the test section. Q_{tfm} need not to be considered in the simulation. All simulations should have temperature at the FPS inlet ($T_{in,FPS}$) of the value tabulated in table II. This temperature is the average temperature at $z=0.0$, the start of heating zone.

Table II Integral parameters of the test ADP10. [1]

Test ADP10 Parameter	Steady state 1			Steady state 2		
	Data	σ	σ [%]	Data	σ	σ [%]
\dot{m}_{gas} (Nl/min)	10	0.5	5	0	0	0
\dot{m}_{LBE} (kg/s)	2.56	0.28	11	1.31	0.14	11
$T_{in,FPS}$ [°C]	231.3	1.5		219.5	1.5	
ΔT_{FPS} [°C]	72	0.7	0.9	140.6	0.3	0.2
Q_{nom} [w]	30000	50	0.2	30000	44	0.1
Q_{eff} [w]	27000	1053	3.9	27000	1010	3.7
Q_{pre} [w]	2236	403	18	2339	217	9.3
Q_{tfm} [w]	1915	3	0.2	1644	4	0.3

In [1] the details of the geometric setup of the fuel pins and recommended physical properties of materials are presented. These data are taken from the OECD handbook [2]. Note, that the fuel pin simulators are composed of multiple layers. The outer stainless teal cladding (AISI316L with physical properties in [3]) is followed by an electrical insulating Bohrium Nitride layer [4]. Inside this heat conducting BNi-layer are three more layers corresponding to an Inconel600 (very thin layer, properties for steel are used for Inconel) pipe and an inner copper rod separated by another BNi layer, properties are found in [4]. Time resolved experimental data of all thermocouples is provided in separate excel files not included in the benchmark specification.

III. Numerical Model and results

For the simulation of the benchmark defined above, the previous experience gained at KIT is employed, see [5-8]. In these validation cases experiments for liquid-metal cooled rod bundles are considered.

Fig. 5 shows the used computational domain. It depicts the extent of the fluid domain and the domains for simulation of heater and wrapper. An adiabatic condition is applied thus neglecting heat losses to the environment. Two trials for the simulation of the heater

have been undertaken. In the first run a heat flux is imposed on the inner side of the cladding. This represents a simplified model for a short heater, i.e., excluding preheating in the preconditioning zone. In the second trial full details of the heater layers are simulated as shown in Fig. 5 (right). The fluid domain includes the full preconditioning section. Solid structures representing the rods in the preheat zone are excluded. Conjugate heat transfer to the rods and wrapper is accounted for. The mesh for the short heater case is composed of 49 M (Million) fluid cells and 13 M solid cells (mesh I). The mesh for the long heater case uses 96 M fluid cells and 29 M solid cells for the heater and wrapper (mesh II). See Fig. 6 for cross sections of the used meshes.

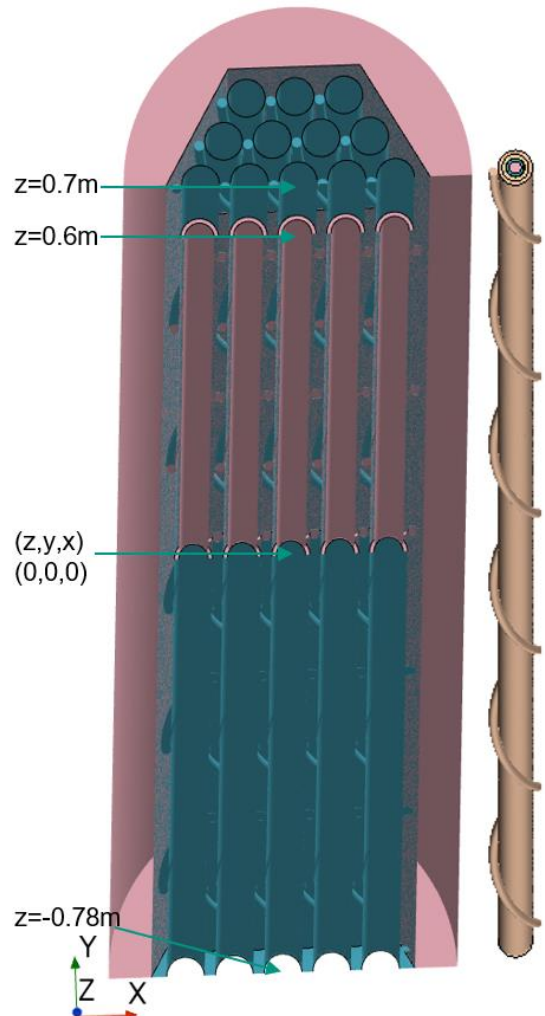


Fig. 5 Computational domain with short, simplified heater (left) and detailed simulated long heater (right).

In this study the flow conditions correspond to the two steady state phases of ADP10 presented in table II are used. The Star CCM+ CFD code is used. The SST

turbulence model with all y^+ wall treatment is selected. Material properties according to the benchmark specifications are used, see upper sections. The gravity effect was accounted for in all the calculations. Temperature dependent physical properties are applied. The inlet condition was set according to table II. For the short heater case the preheating was not considered. Consequently, at the inlet of the computational domain the temperature of the FPS inlet temperature according to table II was set. For the longer heater case the preheating is considered. Accordingly, the inlet temperature was set such that FPS inlet temperature becomes equal to the specified value in table II. For the forced convection case short and long heater tests with their corresponding meshes were tested. For the natural convection case only mesh II and the long heater are considered.

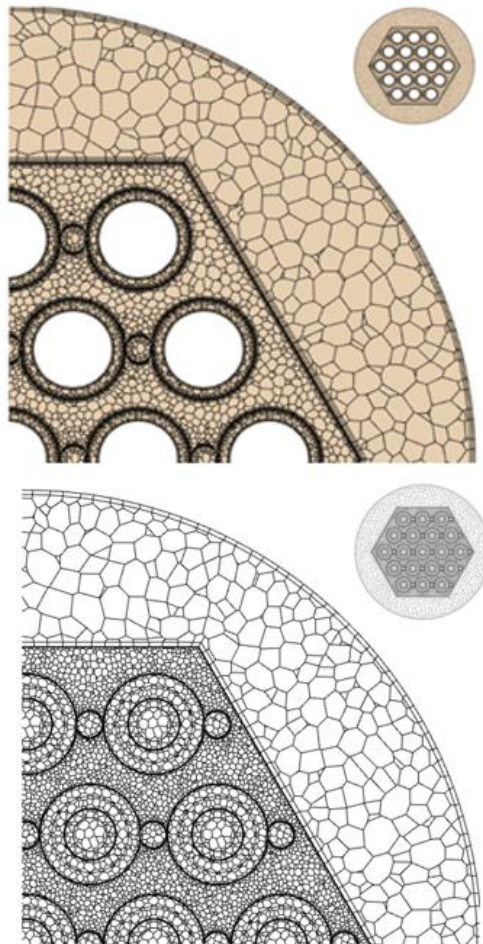


Fig. 6. Cross section of meshes used in simulation. Upper is mesh I and lower is mesh II.

Fig.7 shows the resulting Y^+ values for the steady state case 1 using mesh II. Near similar Y^+ values are preserved for the simulation with mesh I by adjusting the cell size near the walls. The assigned values are suitable for SST and the used wall function treatment.

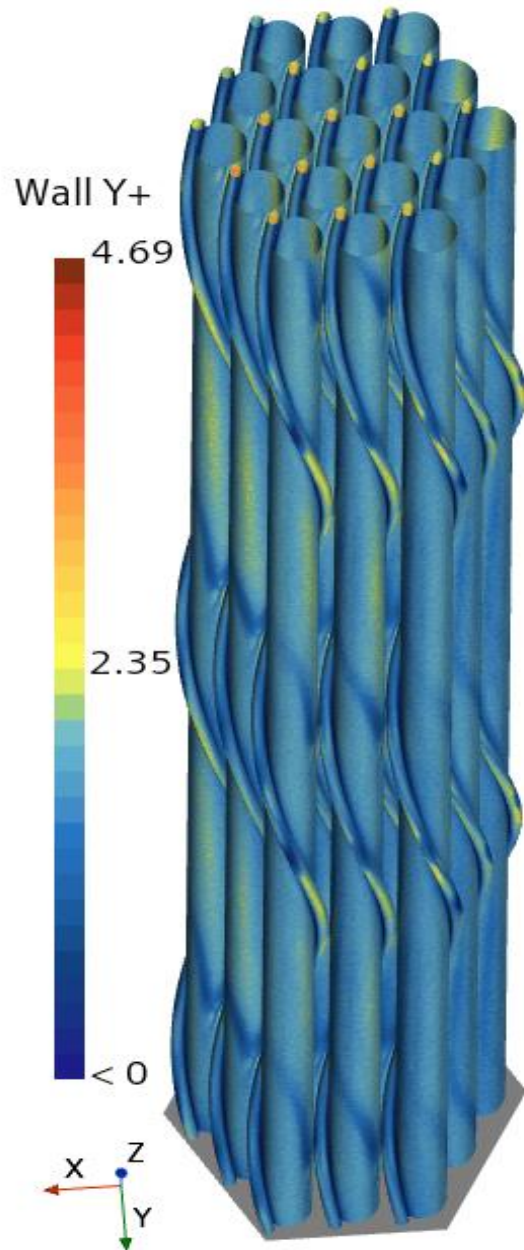


Fig. 7 Y^+ values, mesh II, ADP10 case steady state I.

Fig. 8 shows temperature contours at the heater fluid interface in the heated region ($z=0.0$ to $.0.6$ m) for ADP10 case steady state I and mesh II. The temperature field exhibits a strong temperature gradient in all special directions. Note that the FPS inlet temperature is nonuniform due to the preheating.

Thus, near the wrapper wall lower temperatures than average are obtained. The average inlet temperature of the heated section is $231.3\text{C}=503.45\text{K}$. The scale in Fig. 8 starts from 499 K which is the lowest local temperature in the selected domain.

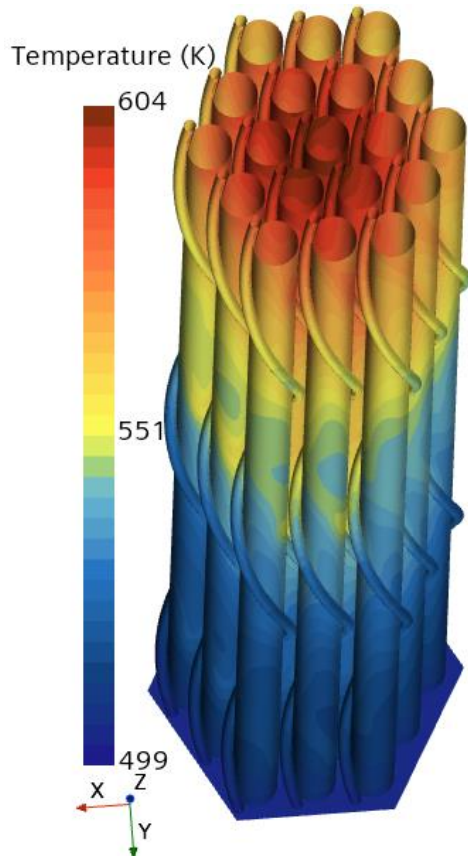


Fig. 8 Temperature contours at heater fluid interface in the heated region, $z=0.0$ to $.06$ m. ADP10 case steady state I, mesh II.

Fig. 9 shows some streamlines originating from a line in the x-y plane (measurement section A, $z=0.038\text{m}$). It highlights strong mixing induced by the wire-wraps. The streamlines are colored by the temperature in their positions.

Local temperature comparisons between benchmark experimental results and simulations are presented in Fig. 10 (forced convection) and Fig. 11 (natural convection). In Fig. 10 and 11 the TC numbers employ the numbering indicated in Fig. 4. TC 1-5, 6-10, and 11-15 measuring fluid temperatures in the subchannels are located in measurement planes A, B, and C, respectively. Similarly, TC 16-28, 29-41, and 42-54 measuring wall temperatures are installed in the planes A, B, and C, respectively. Finally, TC 55-67 represent the wall temperature measurements along

pin 3. They are equally distributed with an axial pitch of 43.7 mm starting from $z=38$ mm.

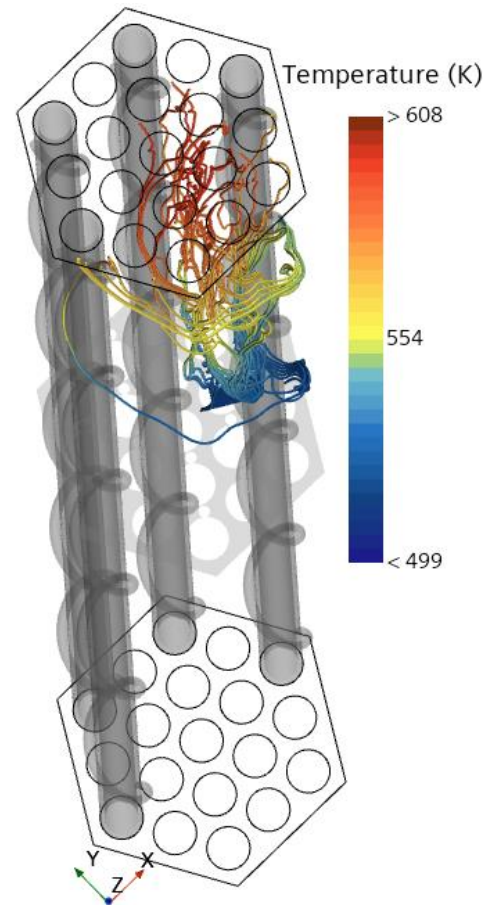


Fig.9 Streamlines originating from a line in x-y plane just downstream of the start of the heated zone, $z=.038\text{m}$, case ADP10 steady state I, mesh II.

Fig. 10 shows the numerical results obtain with the different heater models compared to experiential data. The experimental data have been published and discussed in conference and international journal [9][10][11]. Fig. 10 shows the corresponding experimental results for the steady state case 1 The broken TC number 9 is excluded from the benchmark. The comparison indicates a minimal effect on the numerical results obtained for the short and long cases and even for the more detailed geometry and mesh refinement. Moreover, it proofs a very weak effect when doubling the mesh size. Accordingly, based on the gained experience in the forced convection case, the study of the natural convection case employs mesh II and the long heater geometry. The refined mesh was selected in natural convection simulation for better simulation of the gravitational term, which needs more

cells near heated surfaces than for the forced convection. In Fig. 11 results for the natural convection case are compared to the experimental benchmark results.

Even though, deviations are noticeable at all TCs and between the applied models the deviations are rated as acceptable. This is in particular the case, considering the experimental uncertainties in table II.

In measurement plane A the relative error appears to be quite large. Note, that at this plane the effect of the preconditioning is rather large. Therefore, the actual inlet conditions to the heated section exhibit a large experimental uncertainty. Due to the mixing within the rod bundle this uncertainty becomes less important along the bundle.

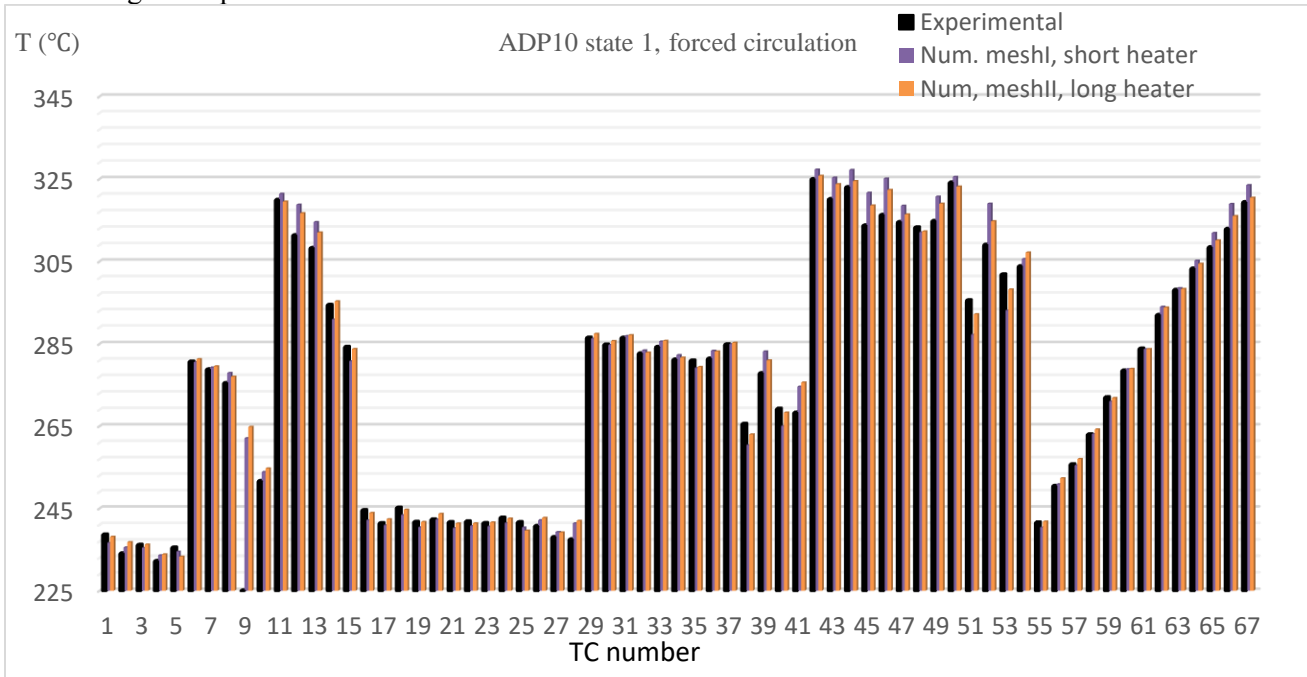


Fig.10 Forced circulation results mesh I with short heater, mesh II with long heater.

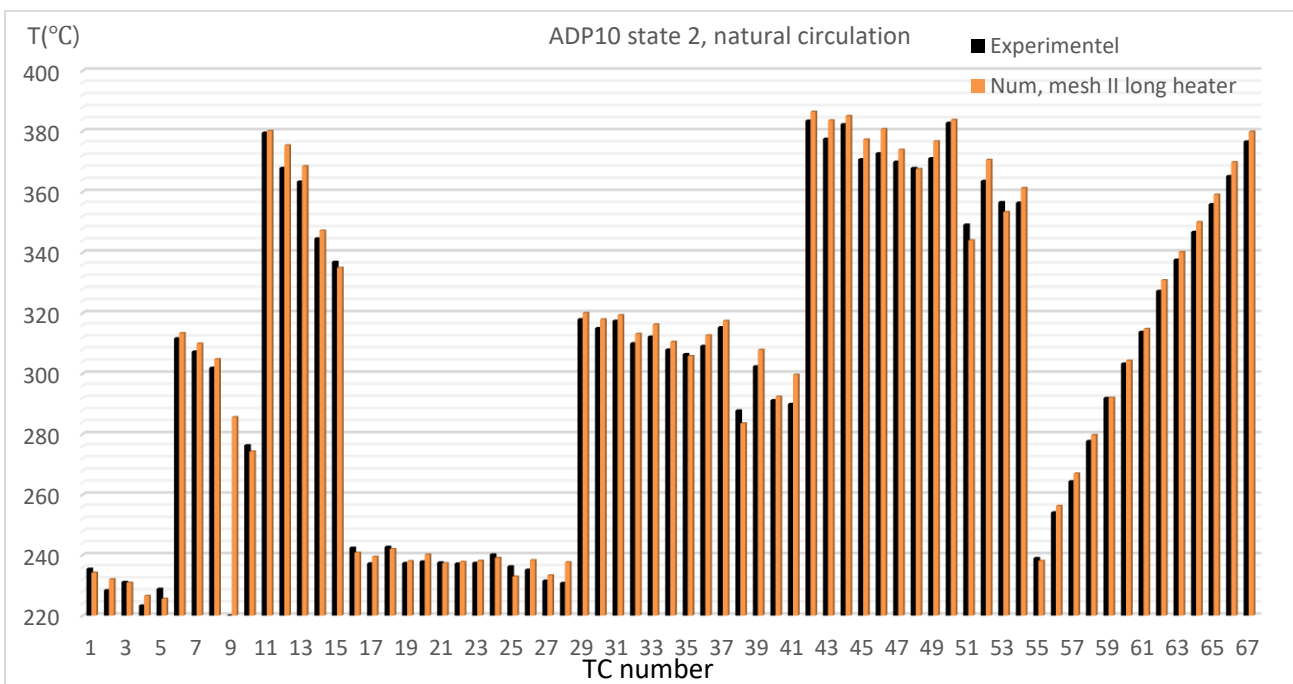


Fig.11 Natural circulation results mesh II with preheating is considered, long heater.

IV. Conclusions

In the open phase of the NACIE -UP benchmark, we were able to test various modelling methodologies. Moreover, we could show less sensitivity of results to mesh refinement. Considering the good quality of our simulations at a relatively low cost, we recommend using the finer mesh and more details in the heater model. When looking at the small differences between the simulations and experiments for the more complex modelling strategy we can still observe slightly better qualitative agreement. This is the main reason, why the more demanding mesh should be employed in the simulations of the blind phase.

We tried various hypothesis to explain systematic deviations between simulation and experiments, including asymmetries and heat losses. None of these could be confirmed by a trend in the data, so that we believe that statistical deviations are dominant and further improvements by more complex models cannot be expected. In regions with high temperatures the uncertainty due to heating power, benchmark specification, and modelling (physical parameters, turbulence models) is dominant. In the inlet region with low temperatures the uncertainty becomes larger as the uncertainty of the boundary conditions becomes more prominent.

Acknowledgments

This work has been supported by the Framatome Professional School at KIT. The data and information presented in the paper are part of an ongoing IAEA coordinated research project on "Benchmark of Transition from Forced to Natural Circulation Experiment with Heavy Liquid Metal Loop – CRP-I31038".

The work presented is original but some or all of the information may need to be included in a book publication at a later date as part of the output of the an International Atomic Energy Agency coordinated research project on "Benchmark of Transition from Forced to Natural Circulation Experiment with Heavy Liquid Metal Loop – CRP-I31038"

References

1. I. Di Piazza, H. Hassan, P. Lorusso, D. Martelli, "Benchmark specifications for nacie-up facility: non-uniform power distribution tests", Ref. NA-I-R-542, Issued: 28/02/2023 ENEA, Italy.
2. N. E. Agency, "Handbook on Lead-bismuth Eutectic Alloy and Lead Properties, Materials Compatibility, Thermal- hydraulics and Technologies," *Nucl. Sci.*, pp. 647–730, 2015.
3. C.S.Kim, "Thermophysical properties of stainless steels", ANL-75-55, 1975.
4. Thermocoax, private communication
5. A. Batta, A. Class, "CFD validation for partially blocked wire-wrapped liquid-metal cooled 19-pin hexagonal rod bundle carried out at KIT-KALLA", Proc. of the 19th International Topical Meeting on Nuclear Reactor Thermal Hydraulics (NURETH-19) Log nr.: 36240 Brussels, Belgium, March 6 - 11, 2022
6. Batta, A. Class, A. Pacio, J. Vlidation for CFD thermalhydraulic simulation for liquid metal cooled blocked 19-pin hexagonal wire wrapped rod bundle experiment carried out at KIT-KALLA, AMNT 50, 2019
7. Batta, A.: Class, A. Thermalhydraulic CFD validation for liquid metal cooled 19-pin hexagonal wire wrapped rod bundle, paper 28473, Nureth 18.
8. Batta, A.: Class, A.; Pacio, J. Numerical analysis of a LBE-cooled blocked 19-pin hexagonal wire wrapped rod bundle experiment carried out at KIT-KALLA within EC-FP7 project MAXSIMA" Paper ID 20532, Nureth 17,
9. R. Marinari, I. Di Piazza, M. Angelucci, D. Martelli, "POST-TEST CFD ANALYSIS OF non-uniformly heated 19-pin fuel bundle cooled by HLM", ICONE26-81307, Proc. ICONE26, July 22-26, 2018, London.
10. M. Angelucci, I. Di Piazza, M. Tarantino, R. Marinari, G. Polazzi, V. Sermenghi, "Experimental tests with non-uniformly heated 19-pins fuel bundle cooled by hlm", ICONE26-81216, Proc. ICONE26, July 22-26, 2018, London.
11. R. Marinari, I. Di Piazza, M. Tarantino, M. Angelucci, D. Martelli, "Experimental tests and post-test analysis of non-uniformly heated 19-pins fuel bundle cooled by Heavy Liquid Metal", *Nucl. Eng. Des.*, Vol. 343, pg. 166-177, 2019